Preparation and Characterization of Polysulfones Containing Both Hexafluoroisopropylidene and Trimethylsilyl Groups as Gas Separation Membrane Materials[†]

Ying Dai,[‡] Michael D. Guiver,*[,‡] Gilles P. Robertson,[‡] Yong Soo Kang,[§] Kwi Jong Lee,[⊥] and Jea Young Jho[⊥]

Institute for Chemical Process and Environmental Technology, National Research Council of Canada, Ottawa, Ontario K1A 0R6, Canada; Center for Facilitated Transport Membranes and Polymer Physics Lab, Korea Institute of Science and Technology, P.O. Box 131, Cheongryang, Seoul 130-650, Korea; and Hyperstructured Organic Materials Research Center and School of Chemical Engineering, Seoul National University, Seoul 151-744, Korea

Received November 19, 2003; Revised Manuscript Received December 16, 2003

ABSTRACT: Trimethylsilylated derivatives of hexafluoropolysulfone (6FPSf) and tetramethylhexafluoropolysulfone (TM6FPSf) were prepared by reaction of lithiated polymer intermediates with halotrimethylsilane electrophiles for a membrane gas separation study to compare improvements in gas permeabilities with those of unmodified polymers. *Ortho* sulfone substituted 6FPSf and TM6FPSf having pendant trimethylsilyl (TMS) groups were obtained by a two-step process involving first direct lithiation of 6FPSf and TM6FPSf solutions with *n*-butyllithium to afford *ortho* sulfone dilithiated intermediates, followed by reaction with a TMS electrophile. The corresponding *ortho* ether 6FPSf derivative was obtained by lithiation of dibrominated 6FPSf at the bromine sites, followed by reaction with a TMS electrophile. The degree of substitution (DS) of the TMS groups was ≥ 2.0 and was dependent on the molar ratio of *n*-butyllithium and electrophile quantity, electrophile reactivity, and reaction conditions. Detailed structural characterization and DS of the modified polymers were obtained by nuclear magnetic resonance spectroscopy. The glass transition temperatures and thermal stabilities were determined by differential scanning calorimetry and thermogravimetric analysis, respectively. Polymer chain *d*-spacing was investigated using wide-angle X-ray diffraction. Polymer free volume was calculated from the polymer density and specific van der Waals volume. The polymer gas permeability coefficients (P) were measured for He, CO_2, O_2, and N_2. Both CO_2 and O_2 permeabilities of modified 6FPSf increased by 8−9-fold ($P(CO_2) = 110$ barrers, $P(O_2) = 28$ barrers) compared with those of the starting polymer 6FPSf ($P(CO_2) = 12$ barrers, $P(O_2) = 3.4$ barrers), which gives P and α properties very close to the upper bound line.[1] Almost no reduction in permselectivity (α) was observed for the CO_2/N_2 gas pair, while the O_2/N_2 gas pair showed moderate reduction.

Introduction

Permeability and permselectivity of polymers significantly depend on the components and structures of polymers. Numerous studies on the relationship between the molecular structure of polymers and their gas transport properties have been reported in an attempt to gain a better understanding of the transport mechanism.[2] The motivation is to improve transport properties by overcoming the "tradeoff" behavior between permeability and permselectivity of polymers, i.e., to increase gas permeability and permselectivity simultaneously. From the material viewpoint, it has been suggested that polymer chain mobility or stiffness and intersegmental distance are two critical factors in determining transport properties, at least for the solution-diffusion mechanism transport in glassy polymers. Typically, chain rigidity imparts increased permselectivity but lower permeability, whereas greater interchain distance imparts higher permeability but lower permselectivity. In terms of polymer molecular design, chain stiffness should be coupled with an increase in interchain separation in order to achieve simultaneously higher permeability and permselectivity.

The presence of bulky silyl groups on the polymer chain is of special interest in membrane gas separation because of their potential to inhibit chain mobility and to give more open chain packing, thus improving both the permselectivity and permeability of a polymer membrane. Gas permeabilities have been shown to be significantly improved by introducing organosilanes onto the polymer main chain[3,4] and postsilylation of polymers. Trialkylsilyl groups introduced onto phenyl rings of polystyrene,[5] on the polypropyne chain,[6−11] and on the phenyl rings of poly(2,6-dimethyl-1,4-phenylene oxide) (PPO)[12−14] and polysulfones[15−18] result in high gas permeability. Many efforts have been made to improve the permeation properties of polysulfones by modifying the chemical structure because aromatic polysulfones such as bisphenol A polysulfone (PSf) and poly(phenyl sulfone) have been widely used for gas separation membranes. PSf has adequate gas separation performance because of its overall combination of relatively high permselectivities and adequate permeabilities to various gases.[1,19,20] In view of its good thermostability, excellent mechanical and fiber spinning properties, and chemical resistance, it was the first commercially available polymer to be used for the fabrication of commercial hollow fiber gas separation membranes for H_2/N_2 and O_2/N_2 separation.[21] Some relevant previous work to the present work has been done whereby parallel families of polysulfones with

---

[†] NRCC No. 46459.

[‡] National Research Council of Canada.

[§] Korea Institute of Science and Technology.

[⊥] Seoul National University.

* Corresponding author. E-mail: michael.guiver@nrc-cnrc.gc.ca.

10.1021/ma035739i CCC: $27.50

systematic structural modifications were correlated with their gas separation properties.[22−28]

Hexafluoropolysulfone (6FPSf) and tetramethylhexafluoropolysulfone (TM6FPSf) are more permeable to many gases than PSf and show less than tradeoff behavior in permselectivity[27,28] because tetramethyl and hexafluoroisopropylidene groups sterically hinder both bond rotation and intersegmental packing. The packing of 6FPSf is further inhibited by intermolecular repulsive forces between fluorine atoms that have high electron density.

In previous work, chemical modification of PSfs was performed in order to study structure−property relationships to improve membrane separation properties. PSf and tetramethylpolysulfone (TMPSf) were activated by direct lithiation[29] or by bromination−lithiation[30] to produce reactive lithiated intermediates that were then converted by various electrophiles to yield the corresponding derivatives.[15,18,31−36] In comparison with previous work in which trimethylsilyl (TMS) groups were introduced on PSf and TMPSf,[15,18,35] this work reports the improvements in gas permeability for 6FPSf and TM6FPSf modified with pendant TMS groups.

Experimental Section

Materials. Hexafluoroacetone gas (97%), 2,6-dimethylphenol (99.5%), and trifluoromethanesulfonic acid (98%) were supplied by Aldrich and were used as received to prepare 3,3′,5,5′-tetramethylhexafluorobisphenol A.[37] 4,4′-Difluorodiphenyl sulfone was supplied by Aldrich and recrystallized from 95% aqueous ethanol. Before polymerization, both monomers were checked as 100% pure by GC-MS and then dried in a vacuum oven at 55 °C for 48 h. 6FPSf[26,27] (inherent viscosity $[\eta]_{\mathrm{inh}} = 0.77$) and TM6FPSf[22,23] ($[\eta]_{\mathrm{inh}} = 0.81$) were made following previously reported synthetic procedures and were dried at 110 °C for at least 24 h before reaction. Reagent grade tetrahydrofuran (THF) was freshly distilled over lithium aluminum hydride ($LiAlH_4$). *n*-Butyllithium (n-C_4H_9Li, 10 M in hexane), bromine, chlorotrimethylsilane (ClTMS), and iodotrimethylsilane (ITMS) were obtained from Aldrich Chemical Co. Lithiation reactions were conducted under a constant argon purge and with mechanical stirring. A mixture of dry ice/ethanol was used for cooling reaction mixtures. All modified polymers were recovered by precipitation from 95% ethanol using a Waring blender, washed thoroughly, and then dried in a vacuum oven at 110 °C.

Preparation of 3,3′,5,5′-Tetramethylhexafluorobisphenol. This monomer was prepared by modifying the procedure of ref 37 as follows. 2,6-Dimethylphenol (36.6 g, 0.30 mol) and CF_3SO_3H (27 g, 15.9 mL, 0.18 mol) were added into a Teflon-lined Parr pressure vessel (125 mL), which was then sealed and cooled with dry ice for 15 min. Meanwhile, hexafluoroacetone gas was cooled to liquid in a cylinder using a dry ice/ethanol mixture. Liquefied hexafluoroacetone (25 mL, 0.15 mol) was measured in a precooled cylinder and added to the autoclave, which was sealed immediately. The autoclave was shaken thoroughly and then warmed to room temperature. It was shaken several times every 10 min. After 6 h it was placed in an oven at 100 °C for about 22 h, and then the autoclave was cooled to room temperature; the resulting brown solid mixture was added into ice water, extracted with diethyl ether twice, and then washed with aqueous sodium bicarbonate until pH = 7. The ether fraction was treated with decolorizing charcoal, then dried over magnesium sulfate, and filtered. Ether was removed by evaporation. A crude light brown product (57.7 g; yield 98% based on hexafluoroacetone conversion) was obtained. The obtained monomer was purified by recrystallized with ethyl acetate/hexane and then sublimed under vacuum at 180 °C. The pure yellow crystal monomer 3,3′,5,5′-tetramethylhexafluorobisphenol (yield, 90%) was obtained [^1H NMR (DMSO-d_6): Ar−H, singlet, 6.88 ppm, 4H; Ar−CH_3, singlet, 2.16 ppm, 12H; OH, singlet, 8.70 ppm, 2H].

Preparation of 6FPSf-*s*-TMS (*Ortho* Sulfone). A solution of 6FPSf (16.22 g, 29.5 mmol) in anhydrous THF (1 wt %) was cooled to −25 °C under argon, and an molar excess of n-C_4H_9Li (8.54 mL, 85.5 mmol) was injected dropwise by syringe pump over 15 min, during which time changes in the color and viscosity of the reaction solution were observed.[29−31] Following addition, the lithiated 6FPSf solution was stirred for 15 min at −25 °C. ClTMS (16.0 g, 18.7 mL, 147 mmol) was injected promptly into the reaction solution, which immediately became less viscous and dark-red, and then the solution was stirred with gradual warming to 0 °C for about 1 h. The polymer was recovered, and the resulting white product (19.1 g; yield 93% calculated from the formula 6FPSf-TMS_2) had a degree of substitution (DS) of 2.0.

Synthesis of 6FPSf-*o*-TMS (*Ortho* Ether). A solution of dibrominated 6FPSf (6FPSf-Br_2)[36] (8.3 g, 11.73 mmol) in THF (1.3 wt %) was cooled to −76 °C under argon, and n-C_4H_9Li (2.6 mL, 25.8 mmol) was injected dropwise by syringe pump over 15 min, during which time changes in the color and reaction solution viscosity were observed. Following addition, the reaction mixture was stirred for an additional 15 min, and then ITMS (7.5 g, 5.3 mL, and 37.5 mmol) was injected promptly into the reaction solution. The solution was stirred with gradual warming to −10 °C. The polymer was recovered by precipitation, washed, and dried in an oven. The white product (7.75 g, yield, 95%, calculated from the formula 6FPSf-TMS_2) had a DS of 2.0. The residual bromine content was 2.98% by elemental analysis.

Synthesis of 6FPSf-TMS. A solution of 6FPSf-Br_2 (6.0 g, 8.48 mmol) in anhydrous THF (1.0 wt %) was cooled to −72 °C under argon, and an excess of n-C_4H_9Li (4.2 mL, 42.4 mmol) was injected dropwise by syringe pump over 15 min. Following addition, the reaction mixture was stirred for an additional 15 min. The solution was warmed to −40 °C, and then ITMS (8.49 g, 6.0 mL, and 42.4 mmol) was injected promptly into the reaction solution. The solution was stirred with gradual warming to −10 to −5 °C and then stirred for 1 h. The polymer was recovered, and the resulting white product (6.13 g; yield, 87%, calculated from the formula 6FPSf-$TMS_{3.55}$) had a DS of 3.55.

Synthesis of TM6FPSf-*s*-TMS (*Ortho* Sulfone). A solution of TM6FPSf (8.0 g, 13.19 mmol) in anhydrous THF (1.0%) was cooled to −45 °C under argon, and n-C_4H_9Li (4.1 mL, 41.5 mmol) was injected dropwise by a syringe pump over 15 min. Following the addition, the reaction mixture was stirred for 30 min, and then ITMS (9.24 g, 6.6 mL, and 46.2 mmol) was injected promptly into the −45 °C reaction solution, which immediately became clear yellow. The solution was stirred with gradual warming to −5 °C and continued to be stirred for 3 h. The polymer was recovered, and the white product (7.78 g; yield 83% calculated from the formula TM6FPSf-$TMS_{1.5}$) had a DS of 1.5.

Synthesis of TM6FPSf-Br_2. Excess bromine (32 mL, 99 g, 0.62 mol) was added to a magnetically stirred solution of TM6FPSf (5.0 g, 8.24 mmol) in chloroform (40 mL) at room temperature and under an argon atmosphere. The dark red homogeneous mixture was stirred at room temperature for 1 week. The polymer was precipitated using methanol. The recovered polymer was left standing in fresh methanol to leach out residual bromine, then filtered again, and dried in a vacuum oven at 55 °C for 24 h. White TM6FPSf-Br_2 (5.20 g; yield, 85% calculated from the formula TM6FPSf-Br_2) polymer was recovered. Elemental analysis: calcd for $C_{31}H_{22}Br_2O_4SF_6$, 21.41% Br; found, 21.09% Br.

Characterization Methods. Nuclear magnetic resonance spectra were recorded on a Varian Unity Inova spectrometer at a resonance frequency of 399.961 MHz for ^1H and 100.579 MHz for ^{13}C. Polymer samples were prepared using $CDCl_3$ as the NMR solvent, and the chloroform signals were used as the chemical shift reference (^1H C*H*Cl_3 7.25 ppm, ^{13}C *C*DCl_3 77.00 ppm). 2D carbon−hydrogen correlation (HETCOR) spectra were recorded for one-bond ^1J C−H (140 Hz) and three-bond ^3J C−H (7.5 Hz) spin correlations. The intrinsic viscosities of polymers in NMP at 35 °C were determined using an Ubbelohde viscometer. The DSs of modified polymers were readily

Scheme 1. Synthesis of 6FPSf-*s*-TMS

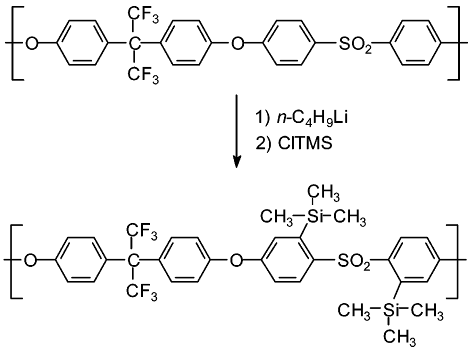

determined using ^{1}H NMR by comparative integration of selected signals (described later). Polymer thermal degradation curves were obtained from thermogravimetric analysis (TGA) (TA Instruments model 2950). Polymer samples for TGA were preheated to 60 °C for 2 h inside the TGA furnace for moisture removal under nitrogen gas and then heated to 600 °C at 10 °C/min for degradation temperature measurement. Glass transition temperatures (T_g) were obtained from differential scanning calorimetry (DSC) (TA Instruments model 2920), and samples for DSC were heated initially to at least 30 °C above T_g at 10 °C/min under a flow of 50 mL/min of nitrogen gas, quenched with liquid nitrogen, and reheated at 10 °C/min for the T_g measurement.

Wide-angle X-ray diffraction (WAXD) was used to investigate *d*-spacing. A Macscience model M18XHF22 was utilized with Cu Kα radiation of wavelength (λ) 1.54 Å, and the scanning speed was 5 °/min. The value of the *d*-spacing was calculated by means of Bragg's law ($d = \lambda/2 \sin \theta$), using θ of the broad peak maximum. Polymer density was determined by the displacement method using a Mettler density kit with anhydrous ethanol at 23 ± 0.1 °C.

Dense polymer films for gas permeability measurements were made from 5 wt % polymer solutions in anhydrous THF that were filtered through 1 μm poly(tetrafluoroethylene) filters, then poured into flat-glass dishes, and dried under a nitrogen atmosphere at room temperature. The detached films were further dried for 3 days in a vacuum oven at 40 °C to remove the residual solvent and then annealed at 130 °C for 4 h. Optically clear films were obtained with a thickness of about 40 μm in all cases. The absence of residual solvent in the films was confirmed by observing T_g using DSC. Permeability coefficients (P) of helium, carbon dioxide, oxygen, and nitrogen were measured by the constant volume method at 35 °C with an upstream pressure of 1 atm.

Results and Discussion

Synthesis. The preparation and purification of monomer 3,3′,5,5′-tetramethylhexafluorobisphenol was by modifying the procedure of ref 37, particularly in the following two steps. Hexafluoroacetone gas was liquefied by passing the gas through a cooling coil immersed in a dry ice/ethanol mixture. The resulting hexafluoroacetone liquid was measured in a dry bag and added quickly to a precooled Parr pressure vessel containing 2,6-dimethylphenol, and then the vessel was sealed immediately to minimize gas loss. After reaction, the recovered crude monomer was purified. The monomer purity is crucial for preparing high molecular weight polymers. The crude monomer was initially treated with decolorizing charcoal in ethyl acetate solution, purified by recrystallization from ethyl acetate/hexane, and then finally sublimed under vacuum at 180 °C to yield pure monomer by GC/MS analysis.

Pendant TMS substituents were introduced onto a series of 6FPSf and TM6FPSf polymers. Scheme 1 shows the chemical modification pathway in which 6FPSf was lithiated directly by 2.9 mol equiv of n-C_4H_9-Li (0.9 mol equiv excess) to afford a THF-soluble intermediate with lithiation geometry regiospecifically around the *ortho* sulfone (-*s*-) site.[36] For the direct lithiation of 6FPSf, an additional ~1 mol equiv of n-C_4H_9Li is required since it is appears that the direct lithiation reaction competes with a complex formed between n-C_4H_9Li and the 6F moiety. In general, dilithiated intermediates were prepared for conversion to TMS derivatives to give the highest DS by the direct lithiation route. The electrophile ClTMS was subsequently reacted under the right temperature conditions with the *ortho* sulfone dilithiated intermediates to yield the corresponding fully substituted TMS-modified polymers with a DS of 2.0.

Scheme 2. Synthesis of 6FPSf-*o*-TMS

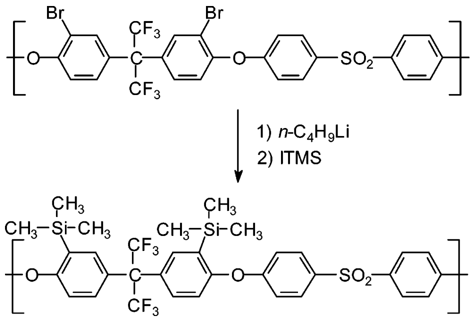

Scheme 3. Synthesis of 6FPSf-TMS

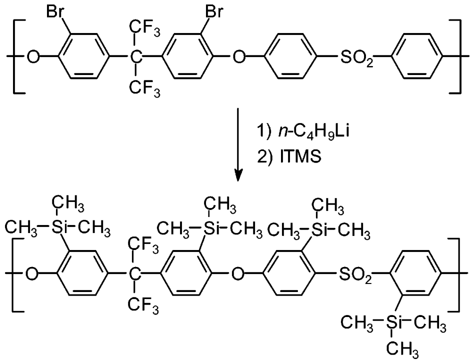

A bromination–lithiation reaction was used to difunctionalize 6FPSf-Br_2 *ortho* to the ether linkage, as described previously.[36] The 6FPSf-Br_2 polymer was first reacted with 2.2 mol equiv of n-C_4H_9Li followed by reaction with the electrophile ITMS to produce a TMS derivative with DS 2.0, as outlined in Scheme 2. Lithium–bromine exchange *ortho* ether (-*o*-) site is by far the most predominant reaction over direct lithiation at the *ortho* sulfone site. The elemental analysis for bromine (2.98%) indicated that only ~13% of bromine remained unexchanged. Minimal amounts of lithium substitution occurred at the (-*s*-) site because the bromine on the bisphenol portion of the polymer chain assists in deactivating the (-*s*-) site, so that a lithium–bromine exchange is the predominant reaction. The reactivity of the electrophile was found to influence DS. For some reactions, 3 mol equiv of ITMS resulted in a DS of 2.0, whereas 5 mol equiv of ClTMS resulted in a DS of only 1.5. The ITMS is more reactive due to the relative reactivity of the leaving groups.

Scheme 3 shows the chemical modification pathway in which 6FPSf-Br_2 was lithiated by an excess of n-C_4H_9-Li (5 mol equiv) to afford a THF-soluble intermediate with lithiation geometry around both the (-*s*-) and (-*o*-)

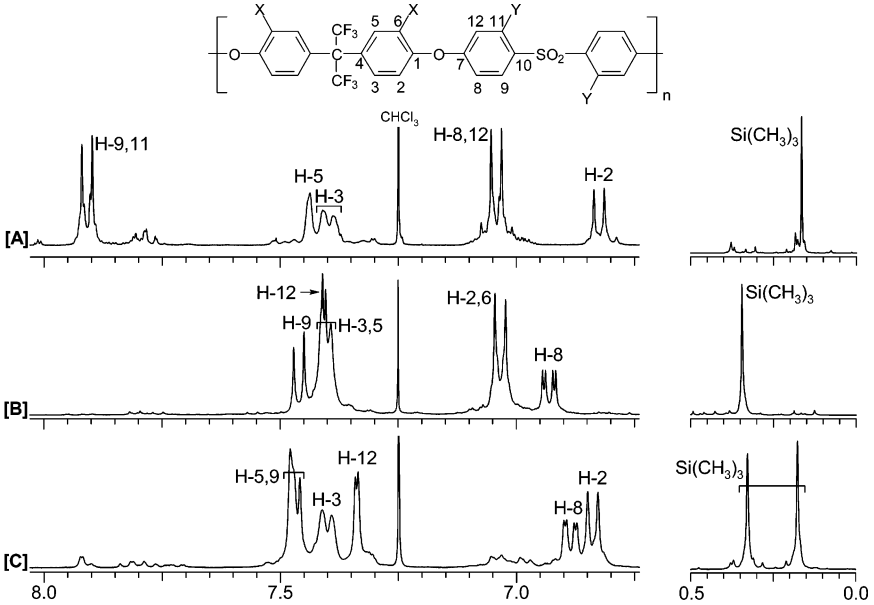

Figure 1. ^{1}H NMR spectra of TMS-substituted 6FPSf: (A) *ortho* ether DS 2 (X,X = TMS; Y,Y = H); (B) *ortho* sulfone DS 2 (X,X = H; Y,Y = TMS); (C) combined *ortho* ether and *ortho* sulfone DS 3 (X,X = TMS; Y,Y = TMS,H).

Scheme 4. Synthesis of TM6FPSf-*s*-TMS

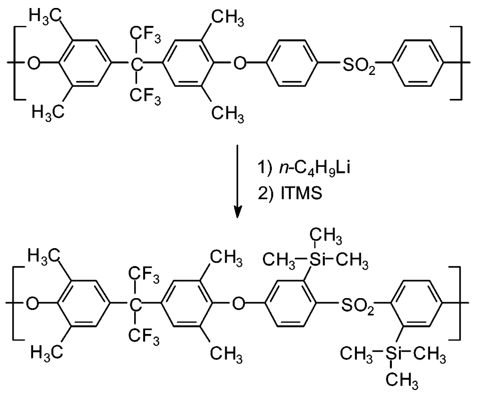

Scheme 5. Synthesis of TM6FPSf-Br$_2$

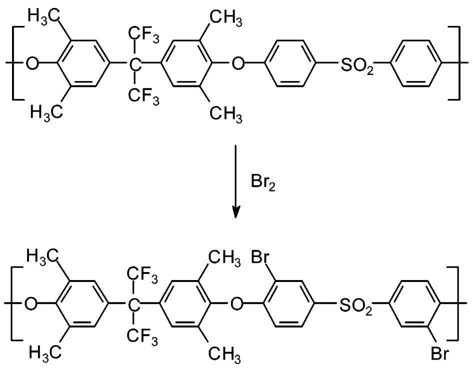

site in order to achieve the maximum amount of substitution on the polymer chain. The resulting TMS polymer had a DS of 3.55.

Scheme 4 shows the chemical modification pathway in which TM6FPSf was lithiated directly by 3.1 mol equiv of *n*-C_4H_9Li to afford a THF-soluble intermediate lithiated at the (-*s*-) site. A polymer with a lower DS of 1.5 was obtained since the presence of the tetramethyl group made the polymer less reactive due to the electron-donating properties and steric hindrance of the symmetrically placed methyl groups.

Scheme 5 shows the chemical modification pathway in which TM6FPSf was brominated. In contrast with TMPSf[18] and 6FPSf,[36] bromination occurred on the *ortho* ether rather than the sulfone site. This is because of the combined influence of the steric hindrance and electronic effects of the 6F and TM moieties. A TMS-modified polymer derived from TM6FPSf-Br$_2$ was not prepared.

Structural Characterization (NMR). As shown before in Schemes 1, 2, and 3, the TMS derivatives of 6FPSf were synthesized by lithiation reaction performed on 6FPSf and 6FPSf-Br$_2$. The spectral analysis for both of 6FPSf and 6FPSf-Br$_2$ was reported previously.[36] Figure 1 shows ^{1}H NMR stacked spectra of three 6FPSf TMS derivatives along with complete assignment for all of the signals. Assignment of the aromatic hydrogen signals is based on the results of simple homonuclear decoupling experiments performed on every proton frequency. Unsubstituted phenylene rings present in both DS 2 6FPSf-*o*-TMS and 6FPSf-*s*-TMS (Figure 1A,B) show two signals of intensity 4H along with a typical 8.8 Hz spin−spin coupling between the two adjacent aromatic hydrogen atoms. Analogously, the aromatic signals of TMS substituted phenylene rings of all three derivatives in Figure 1 show the characteristic multiplicity resulting from spin−spin coupling between hydrogen atoms at the *ortho* and *meta* positions. For example, the doublet of doublets H-8 (6.93 ppm) of 6FPSf-*s*-TMS in Figure 1B has a three-bond coupling (8.8 Hz) with H_9 (7.46 ppm) and also a four-bond coupling (2.0 Hz) with H_{12} (7.40 ppm). The considerable 0.5 ppm shift toward lower frequency of H-9 (7.46 ppm) from 6FPSf-*s*-TMS compared with H-9 from TM6FPSf-*o*-TMS (7.91 ppm) is due to the shielding effect of the bulky electron-rich TMS group of the opposite phenylene ring. The methyl signals arising from the TMS groups at the *ortho* ether and *ortho* sulfone positions are also displayed in the low-frequency NMR region of Figure 1A−C.

The ^{1}H NMR spectrum of TM6FPSf displayed in Figure 2 is simple and unambiguous. The spectrum is composed of three aromatic signals: a singlet of intensity 4H for the bis-phenol chemically equivalent meta-ether protons (H_{3-5}) and two coupled (8.0 Hz) doublet

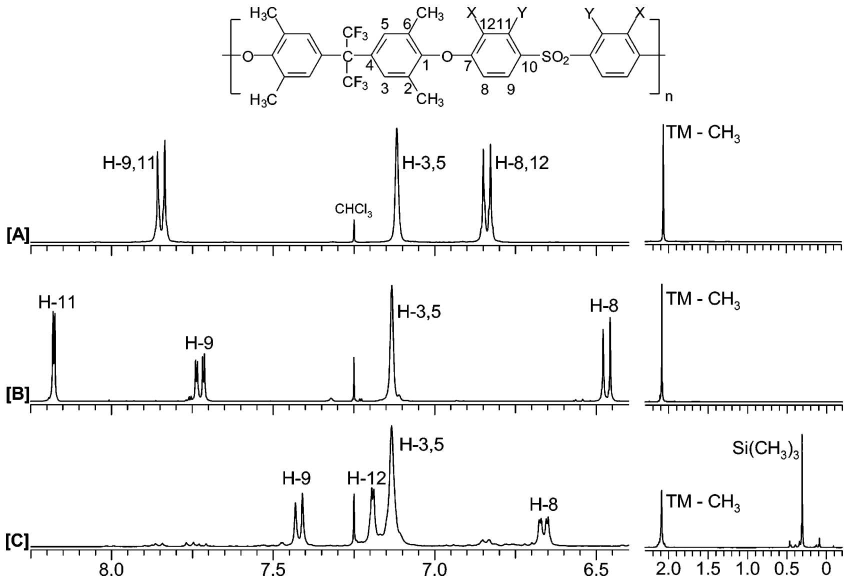

Figure 2. ^{1}H NMR spectra of (A) TM6FPSf (X,X = Y,Y = H), (B) brominated TM6FPSf (X,X = Br; Y,Y = H), and (C) TMS-substituted TM6FPSf (X,X = H; Y,Y = TMS).

Table 1. ^{13}C NMR Chemical Shifts of 6FPSf and TM6FPSf Derivatives (^{1}H Noise Decoupled)

carbon no.	6FPSf-TMS$_2$ DS 2 (-*o*-) (ppm)	6FPSf-TMS$_2$ DS 2 (-*s*-) (ppm)	TM6FPSf (ppm)	TM6FPSf-Br$_2$ DS 2 (-*o*-) (ppm)	TM6FPSf-TMS$_2$ DS ~2 *ortho* (-*s*-) (ppm)
C1	160.37	156.16	150.68	150.73	150.72
C2	118.00	119.26	130.65	130.84	131.01
C3	132.71	132.04	131.01	131.09	130.90
C4	129.16	129.20	130.99	131.09	130.54
C5	137.73	132.04	160.84	131.09	130.90
C6	131.52	119.26	130.65	130.84	131.01
C7	161.13	159.22	160.84	157.36	159.19
C8	118.44	117.63	115.23	113.90	114.09
C9	129.98	131.53	129.99	128.65	131.57
C10	136.03	141.55	134.96	135.66	139.98
C11	129.98	143.70	129.99	133.37	143.25
C12	118.44	126.52	115.23	112.17	122.81
CF3-*C*-CF3	63.93 (sept, *J* 25.4)	63.93 (sept, *J* 25.4)	63.98 (sept, *J* 25.3)	63.98 (sept, *J* 25.3)	64.09 (sept, *J* 26.0)
CF3	124.15 (q, *J* 285.4)	124.10 (q, *J* 285.1)	124.09 (q, *J* 285.4)	124.01 (q, *J* 285.4)	124.08 (q, *J* 284.1)
Ar−CH3			16.55	16.44	16.71
Si(CH3)3	−1.16 (s)	0.98 (s)			1.04

signals for *ortho* sulfone protons H_{9-11} (7.85 ppm) and *meta* sulfone protons H_{8-12} (6.84 ppm). Also displayed in Figure B,C are the brominated and TMS derivatives of modified TM6FPSf. The NMR spectrum of the brominated derivative shows that reaction occurred exclusively at the *meta* sulfone sites of the sulfone segment. As a result of that, no impact on the chemical shift of the singlet H_{3-5} was observed. The characteristic three-spin system resulting from three-bond and four-bond aromatic coupling of H-9 with H-8 and H-11 is clear. The combined electron-withdrawing effects of sulfone and bromine functionalities had a deshielding repercussion on H-11, consequently shifting it to higher frequency. On the other end, the lower frequency shift of H-8 can be explained by 3-d conformation resulting from steric hindrance. The bulky bromine atom restricts the rotation of the phenylene rings about nonlinear ether linkage, forcing H-8 to be situated closer to the electron inductive methyl groups and also possibly on top of the phenylene ring where annular ring current would also shield the hydrogen atom and shift it to lower NMR frequency. The spectral characteristics of the aromatic region of Figure 2C from TM6FPSf-*s*-TMS resemble those of similar derivatives described before (H-3,5 singlet, three-spin system H-8,9,12, H-9 shift to lower frequency). The methyl signals arising from the tetramethyl and the TMS groups are also displayed in the low-frequency NMR region of Figure 2A−C.

Table 1 is an exhaustive list of the carbon frequency for the 6FPSf and TM6FPSf derivatives. The signals were unambiguously assigned from 2D carbon−hydrogen heteronuclear correlation (^1J C−H, ^3J C−H) spectra.

The DS of the TMS-substituted TM6FPSf was readily determined by comparing the signal intensities of the distinct low-frequency trimethylsilyl signal with that of the four aromatic methyl groups. The DS of the 6FPSf TMS derivatives was estimated by comparing the intensity of the low-frequency TMS signal with the totality of the aromatic signal integration. The simplicity of the spectra aromatic regions suggests that the polymer derivatives are disubstituted (Figure 1A,B) and trisubstituted (Figure 1C).

Physical Properties. Table 2 lists the T_gs and actual onset temperatures of degradation (for 1% weight loss) of 6FPSf and TM6FPSf and their Br and TMS derivatives. The TGA curve of 6FPSf had a very similar, almost overlapping curve compared with PSf (not shown), which indicated that carbon−fluorine bonds or carbon−hydrogen bonds at the isopropylidene group do not make an important difference in terms of thermal stability of the polymers. The TM6FPSf polymers were

Table 2. Glass Transition Temperatures and Onset Temperatures of Thermal Degradation of 6FPSf, TM6FPSf, and Their Derivatives

polymer structure	DS	T_g, °C	actual onset, °C	extrapolated onset, °C
6FPSf		199.4	489.0	510.9
6FPSf−Br_2	2	197.5	464.3	501.8
6FPSf-*o*-TMS	2.0	168.6	397.62	379.09
6FPSf-*s*-TMS	2.0	172.0	376.1	428.4
6FPSf-TMS	3.5	148.9	388.0	440.6
TM6FPSf		235.5	424.4	430.3
TM6FPSf−Br_2	1.5	230.8	286.4	338.8
TM6FPSf-*s*-TMS	1.5	197.0	323.1	414.4

thermally not as stable as the 6FPSf polymers. The methyl groups appear to have a weakening effect on the thermal stability of the bisphenol phenylene rings, making the polymer more susceptible to degradation at temperatures above 300 °C. The TMS derivatives of 6FPSf and TM6FPSf are comparatively less stable thermally than the unmodified polymers because of the weaker C−Si bond, but their onset temperatures of thermal degradation are adequate (the minimum value is 280 °C). Note that *ortho* ether TMS derivatives of 6FPSf have almost the same thermal stability as the corresponding *ortho* sulfone derivatives, in contrast with the behavior of TMS derivatives of PSf.[15] This may be due to both the bisphenol-6F rings and the sulfone groups being sterically hindered and containing strongly electron-withdrawing sulfone and 6F groups.

All the TMS derivatives of 6FPSf and TM6FPSf have lower T_gs than the respective unmodified polymers, suggesting a breakage in symmetry of the phenylene ring by the introduction of TMS groups. When comparing the T_gs of the individual 6FPSf derivatives, the dibrominated derivative has a T_g virtually unchanged, while the TMS derivative has a substantially reduced T_g by about 30 °C. This suggests that the TMS groups have the effect of reducing chain stiffening on the polymer backbone. As expected, the T_g of TM6FPSf is considerably higher than the other polymers (235 °C) because of the chain stiffening introduced by the four aromatic methyls. Similarly to what was observed in the 6FPSf, the introduction of bromine onto TM6FPSf resulted in only a small reduction in T_g, while TMS groups had a reduction of the T_g by as much as 37 °C.

The *d*-spacings of 6FPSf and TM6FPSf and their TMS derivatives were calculated from WAXS spectra by Bragg's law and are listed in Table 3. The *d*-spacings of all TMS derivatives increased with the DS as expected. In particular, TM6FPSf-*s*-TMS has the highest *d* spacing value of 6.3 Å. The increased *d*-spacing may be explained by a suppression or disruption of chain packing by the asymmetric substitution of serially bulky but mobile TMS groups. This is consistent with previous results that indicated that the substituent mobility rather than its size correlates well with the *d*-spacing and consequently with gas permeability. The disrupted chain packing is also validated by the fractional free volume (FFV) and the packing density (PD). FFV was calculated using the following relationship:[38]

$$V_\mathrm{f} = V_\mathrm{sp} - 1.3V_\mathrm{w}$$

$$\mathrm{FFV} = V_\mathrm{f}/V_\mathrm{sp}$$

whereV_f is the free volume, V_sp is the specific volume, and V_w is the specific van der Waals volume, calculated using the group contribution method of Bondi.[39,40] PD was calculated using[41]

$$\mathrm{PD} = V_\mathrm{sp}/(V_\mathrm{sp} - V_\mathrm{w})$$

PD and FFV data are also listed in Table 3. The results are consistent with those of the *d*-spacing. In other words, the larger the *d*-spacing is, the larger FFV and the smaller PD are, and vice versa. Therefore, it is apparent that the TMS group is effective in disrupting chain packing, which is directly correlated with gas permeability.

Gas Transport Properties. A tradeoff relationship is usually observed between P and α for common gases in glassy or rubbery polymers. That is higher permeability is gained at the cost of permselectivity and vice versa. The basic principle for overcoming this tradeoff behavior so as to achieve simultaneously higher permeability and permselectivity is that the polymer chain stiffness should be maintained while increasing with the interchain separation. It is important to note that this is true only if the increased chain separation allows tight control of the free-volume distribution which results from the separation of the chains. If the free-volume distribution is broadened as the chains are separated, a loss in selectivity will also be observed.

On this basis, a series of bulky but mobile TMS groups were introduced onto the polymer chains.

The experimental gas permeability data for O_2/N_2 and CO_2/N_2 are presented graphically in Figures 3 and 4, respectively. The dashed and solid lines in the figures represent the upper bound lines of Robeson[1] and Park et al.,[19] respectively. The point on the upper bound lines in Figures 3 and 4 refers to poly(tetrabromofluorene tetrabutyl isophthalate),[19] known to have the best combined $P-\alpha$ value for both O_2/N_2 and CO_2/N_2 gas pairs. The distance (δ) from the permeability point (P_i vs α_{ij}, where permselectivity $\alpha_{ij} = P_i/P_j$) to the upper bound line was calculated by the method developed previously.[36] Table 4 lists P, α, and δ values for 6FPSf, TM6FPSf, and their derivatives. The polymer permeability coefficients decrease in the following order: He > CO_2 > O_2 > N_2 > CH_4, which is also the order of increasing kinetic diameters of the gases.

Upon incorporation of TMS groups in main chains, $P(O_2)$ increased significantly with some decrease in $\alpha(O_2/N_2)$ as observed previously.[35] For the O_2/N_2 gas pair, the lowest δ value of 0.082 was obtained for 6FPSf-TMS having the highest degree of substitution of 3.55, indicating the importance of the DS to inhibit chain

Table 3. Physical Properties of 6FPSfs

polymer	*d*-space (Å)	ρ (g/cm^3)	V_sp (cm^3/g)	M (g/mol)	V_w (cm^3/mol)	V_f (cm^3/g)	PD	FFV
6FPSf	5.1	1.43	0.70	550.47	250.4	0.109	2.86	0.155
6FPSf-*s*-TMS	5.3	1.27	0.79	694.84	358.74	0.125	2.85	0.157
6FPSf-*o*-TMS	5.4	1.25	0.80	694.84	358.74	0.129	2.82	0.161
6FPSf-TMS	5.4	1.16	0.86	803.10	440.00	0.148	2.76	0.172
TM6FPSf	5.3	1.32	0.76	606.58	295.00	0.123	2.81	0.163
TM6FPSf-*s*-TMS	6.3	1.20	0.83	714.85	376.26	0.146	2.73	0.176

Table 4. Gas Permeabilities of Modified 6FPSfs

	P (barrers)[a]				α[b]				$\delta \times 10^3$ (Å)			
polymer	He	CO_2	O_2	N_2	O_2/N_2	CO_2/N_2	He/CO_2	He/N_2	O_2/N_2	CO_2/N_2	He/CO_2	He/N_2
6FPSf	33	12	3.4	0.67	5.1	18	2.8	49	187	373	531	514
6FPSf-*s*-TMS	62	41	9.9	2.0	4.8	20	1.5	31	126	154	587	456
6FPSf-*o*-TMS	97	84	20	4.7	4.3	18	1.2	21	126	102	571	438
6FPSf-TMS	150	110	28	6.3	4.4	18	1.4	24	82	73	404	259
TM6FPSf	113	72	18	4.0	4.5	18	1.6	24	110	120	424	296
TM6FPSf-*s*-TMS	127	96	23	5.2	4.4	19	1.3	25	101	65	456	300

[a] Permeability coefficients measured at 35 °C and 1 atm pressure. 1 barrer = 10^{-10} [cm^3 (STP) cm]/(cm^2 s cmHg). [b] Ideal permselectivity $\alpha = P_a/P_b$.

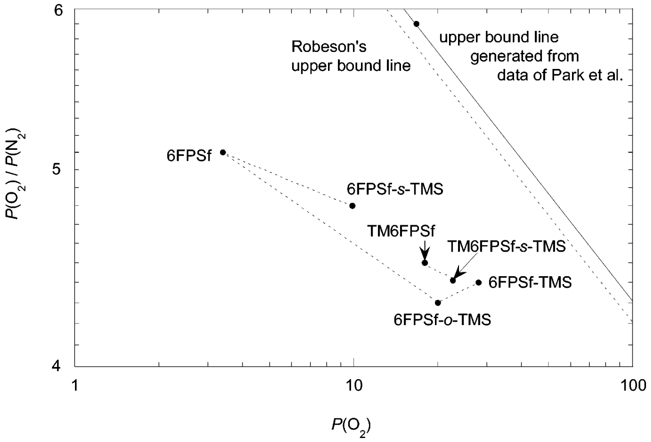

Figure 3. Gas separation properties of modified 6FPSfs and TM6FPSfs for O_2 and N_2 in relation to the upper bound lines of Robeson[1] (dashed line) and Park et al.[19] (solid line).

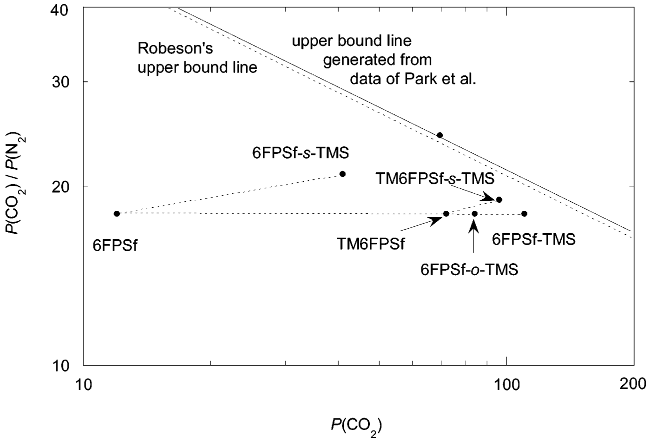

Figure 4. Gas separation properties of modified 6FPSfs and TM6FPSfs for CO_2 and N_2 in relation to the upper bound lines.

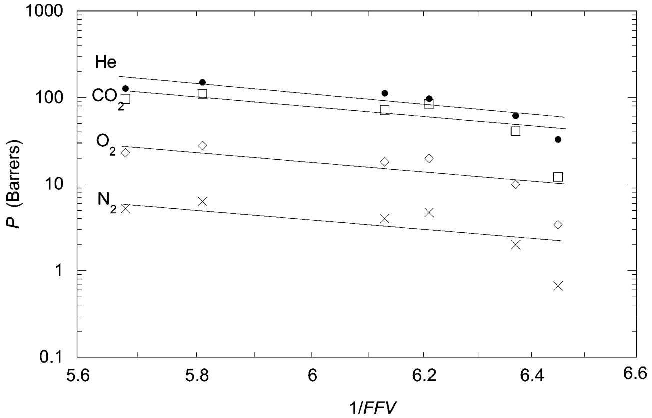

Figure 5. Logarithmic P as a function of reciprocal FFV at 35 °C and 1 atm upstream pressure.

packing. TMS substitution of 6FPSf at the (-*o*-) site gave comparable data with that of the (-*s*-) site. In the case of CO_2/N_2, the $P(CO_2)$ increased markedly upon TMS incorporation, without sacrificing or with even increasing $\alpha(CO_2/N_2)$ in some cases. Both 6FPSf-TMS and TM6FPSf-TMS gave the $P(CO_2)$ values in the range of 100−110 barrers and the $\alpha(CO_2/N_2)$ of 18−19, which is very close to the upper bound line (δ is 0.06−0.07). The incorporation of TMS groups onto the main chain of these particular polymers is clearly effective in improving the permselectivities to gases without an upper-bound coupled reduction in permabilities, especially for the CO_2/N_2 gas pair. The polymers in this study, from which flexible films could be cast, all fall below the upper bound line, although some polymers lie close to it. The polymers with the most desirable combination of permeability and selectivity (i.e., those closest to the upper bound line for the CO_2/N_2 and O_2/N_2 gas pairs) are 6FPSf-TMS and TM6FPSf-*s*-TMS.

The FFV is closely connected to the diffusion coefficients in a strict sense according to the free-volume theory. However, it has been experimentally found that the permeability can also be similarly correlated with FFV as follows:[24]

$$P = A \exp(-B/\mathrm{FFV})$$

where A and B are parameters. Figure 5 shows that a fairly linear relationship between log(P) vs 1/FFV exists for the TMS-modified polymers for all five gases. The exception for the unmodified polymers could be due to the solubility difference between modified and unmodified polymers because the linear relationship between log(P) and (1/FFV) is based on the identical solubility coefficients.[1,38] This suggests that the increased permeability appears to be closely correlated with an increase in the diffusion coefficient, which is associated with high free volume or low packing density due to TMS substitution.

Conclusions

TMS groups have been systematically introduced onto the main chains of 6FPSf and TM6FPSf on either the bisphenol or phenyl sulfone segments. The chemical structures of the modified polymers were characterized spectroscopically. The O_2 permeability increases significantly up to 28 barrers and 23 from 3.4 and 18 barrers for 6FPSf-TMS and TM6FPSf-*s*-TMS, respectively, upon incorporation of TMS groups, with a moderate decline in permselectivity for O_2/N_2. In the case of CO_2/N_2, the CO_2 permeabilities of 6FPSf-TMS and TM6FPSf-*s*-TMS increase remarkably (up to 100−110 barrers) without a decline in permselectivity, which is very close to the upper bound line. The incorporation of bulky but mobile TMS groups onto the main chain of these particular polymers is clearly effective in improving the permeabilities to gases without an upper-bound coupled reduction in permselectivities, especially for the CO_2/N_2 gas pair. The improved characteristics of the separation performance are believed to be due primarily to the increased diffusion coefficients owing to the disruption of the chain packing by asymmetric substitution of TMS groups, as confirmed by glass transition temperature, *d*-spacing, fractional free volume and packing density. These results suggest that the substitution of TMS groups onto the main chains of polymers already having good gas transport properties is very useful in improving the gas transport properties.

References and Notes

(1) Robeson, L. M. *J. Membr. Sci.* **1991**, *62*, 165.
(2) Pixton, M. R.; Paul, D. R. In *Polymeric Gas Separation Membranes*; Paul, D. R., Yampolskii, Y. P., Eds.; CRC Press: Boca Raton, FL, 1994; Chapter 3, pp 83–153.
(3) Plate, N. A.; Durgarjan, S. G.; Khotimskii, V. S.; Teplyakov, V. V.; Yampol'skii, Yu. P. *J. Membr. Sci.* **1990**, *52*, 289.
(4) Yampol'skii, Yu. P.; Volkov, V. V. *J. Membr. Sci.* **1991**, *64*, 191.
(5) Kawakami, Y.; Karasawa, H.; Aoki, T.; Yamamura, Y.; Hisada, H.; Yamashita, Y. *Polym. J.* **1985**, *17*, 1159.
(6) Masuda, T.; Isobe, E.; Higashimura, T.; Takada, K. *J. Am. Chem. Soc.* **1983**, *105*, 7473.
(7) Ichiraku, Y.; Stern, S. A.; Nakagawa, T. *J. Membr. Sci.* **1987**, *34*, 5.
(8) Masuda, T.; Iguchi, Y.; Tang, B.-Z.; Higashimura, T. *Polymer* **1988**, *29*, 2041.
(9) Ichiraku, Y.; Higuchi, A.; Nakagawa, T. *J. Polym. Sci., Part B: Polym. Phys.* **1995**, *33*, 289.
(10) Madkour, M. *Polymer* **2000**, *41*, 7489.
(11) Nagai, K.; Masuda, T.; Nakagawa, T.; Freeman, B. D.; Pinnau, I. *Prog. Polym. Sci.* **2001**, *26*, 721.
(12) Nagase, Y.; Udea, T.; Matsui, K.; Uchikura, M. *Polym. J.* **1986**, *43*, 733.
(13) Perego, G.; Roggero, A.; Sisto, R.; Valentini, C. *J. Membr. Sci.* **1991**, *55*, 325.
(14) Zhang, J.; Hou, X. *J. Membr. Sci.* **1994**, *97*, 275.
(15) Guiver, M. D.; Robertson, G. P.; Rowe, S.; Foley, S.; Kang, Y. S.; Park, H. C.; Won, J.; Le Thi, H. N. *J. Polym. Sci., Part A: Polym. Chem.* **2001**, *39*, 2103.
(16) Sisto, R.; Bonfanti, C.; Valenti, C. *J. Membr. Sci.* **1994**, *95*, 135.
(17) Lee, K. J.; Jho, J. Y.; Kang, Y. S.; Dai, Y.; Robertson, G. P.; Guiver, M. D. Won, J. *J. Membr. Sci.* **2003**, *212*, 147.
(18) Dai, Y.; Guiver, M. D.; Robertson, G. P.; Bilodeau, F.; Kang, Y. S.; Lee, K.; Jho, J. Y.; Won, J. *Polymer* **2002**, *43*, 5369.
(19) Park, J. Y.; Paul, D. R. *J. Membr. Sci.* **1997**, *125*, 23.
(20) Robeson, L. M.; Smith, C. D.; Langsam, M. *J. Membr. Sci.* **1997**, *132*, 33.
(21) Henis, J. M. S.; Tripodi, M. K. *Sep. Sci. Technol.* **1980**, *15*, 1059.
(22) Mohanty, D. K.; Sachdeva, Y.; Hedrick, J. L.; Wolfe, J. F.; McGrath, J. E. *Polym. Prepr.* (*Am. Chem. Soc., Div. Polym. Chem.*) **1984**, *25*, 19.
(23) Mohanty, D. K. Ph.D. Dissertation, Virginia Polytechnic Institute and State University, 1983.
(24) Aitken, C. L.; Koros, W. J.; Paul, D. R. *Macromolecules* **1992**, *25*, 3424.
(25) Aitken, C. L.; McHattie, J. S.; Paul, D. R. *Macromolecules* **1992**, *25*, 2910.
(26) McHattie, J. S.; Koros, W. J.; Paul, D. R. *Polymer* **1992**, *33*, 1701.
(27) McHattie, J. S.; Koros, W. J.; Paul, D. R. *Polymer* **1991**, *32*, 2618.
(28) McHattie, J. S.; Koros, W. J.; Paul, D. R. *Polymer* **1991**, *32*, 840.
(29) Guiver, M. D.; ApSimon, J. W.; Kutowy, O. *J. Polym. Sci., Polym. Lett Ed.* **1988**, *26*, 123.
(30) Guiver, M. D.; Kutowy, O.; ApSimon, J. W. *Polymer* **1989**, *30*, 1137.
(31) Guiver, M. D.; Robertson, G. P. *Macromolecules* **1995**, *28*, 294.
(32) Guiver, M. D.; Robertson, G. P.; Foley, S. *Macromolecules* **1995**, *28*, 7612.
(33) Guiver, M. D.; Zhang, H.; Robertson, G. P.; Dai, Y. *J. Polym. Sci., Part A: Polym. Chem.* **2001**, *39*, 675.
(34) Guiver, M. D.; Robertson, G. P.; Yoshikawa, M.; Tam, C. M. *ACS Symposium Series 744*; *Membranes Formation and Modification*; Pinnau I., Freeman, B., Eds.; American Chemical Society: Washington, DC, 1999; Chapter 10, p 137.
(35) Kim, I.-W.; Lee, K. J.; Jho, J. Y.; Park, H. C.; Won, J.; Kang, Y. S.; Guiver, M. D.; Robertson, G. P.; Dai, Y. *Macromolecules* **2001**, *34*, 2908.
(36) Dai, Y.; Guiver, M. D.; Robertson, G. P.; Kang, Y. S.; Lee, K.; Jho, J. Y.; Won, J. *Macromolecules* **2003**, *36*, 6807.
(37) Mark, V.; Hedges, C. V. U.S. Patent. 4,358,624, 1982.
(38) Lee, W. M. *Polym. Eng. Sci.* **1980,** *20*, 65.
(39) Bondi, A. *J. Phys. Chem.* **1964**, *68*, 441.
(40) van Krevelen, D. W. *Properties of Polymers: Their Correlation with Chemical Structure; Their Numerical Estimation and Prediction from Additive Group Contributions*; Elsevier: Amsterdam, 1990.
(41) Chern, R. T.; Sheu, F. R.; Jia, L.; Stannett, V. T.; Hopfenberg, H. B. *J. Membr. Sci.* **1987**, *35*, 103.

MA035739I